DOI: 10.1002/ejic.200500947

Zinc Thiolate Complexes $[ZnL_n(SR)]^+$ with Azamacrocyclic Ligands: Synthesis and Structural Properties

Johannes Notni,[a] Helmar Görls,[b] and Ernst Anders*[a]

Keywords: Enzyme models / Macrocyclic ligands / S ligands / Solid-state structures / Zinc

A series of 24 novel zinc thiolate complexes containing saturated macrocyclic polyamine ligands with the general formula $[Zn(L_n)(SR)]ClO_4$ (L_n: *n*-dentate azamacrocyclic ligand) has been synthesized. Two different thiolate ligands (R = phenyl, benzyl) and 12 macrocyclic ligands with ring sizes varying from 11 to 16 atoms and containing three, four, and five nitrogen donors (including a new macrocyclic triamine ligand, 8-methyl-[11]aneN_3) have been used. The solid-state structures of 20 of the 24 complexes have been characterized by X-ray diffraction. The crystal lattice of all compounds is comprised exclusively of monomers. The tetracoordinate N_3S compounds exhibit Zn–S bond lengths ranging from 2.2259(5) to 2.2492(9) Å and the pentacoordinate N_4S systems from 2.266(2) to 2.3200(7) Å. In addition, two complexes with the very rare N_5S coordination environment for zinc have been found. They exhibit Zn–S bond lengths of 2.3782(7) and 2.42 Å (mean value of two independent molecules). The thiolate complexes are suitable model systems for the precursor proteins of matrix metalloproteases (proMMPs) as well as for thiolate alkylating enzymes such as cobalamine-dependent/independent methionine synthases, farnesyl transferase, and the Ada repair protein.

Introduction

Zinc thiolate complexes have received considerable attention in the past decade. This interest derives from the fact that many enzymes feature the alkylation (methylation) of a zinc–thiolate bond.[1,2] The most prominent among them are the Ada repair protein,[3] cobalamine-dependent/independent methionine synthases,[4,5] and farnesyl transferase.[6] The studies focusing on zinc thiolate complexes have thus paid special attention to the mechanism of the alkylation of thiols. Two different possible reaction modes are discussed. On the one hand, the alkylation may occur intramolecularly and the thiol is alkylated in the zinc-bound state, whereas the reaction could also start with an initial heterolytic dissociation, followed by a reaction of free thiolate. Wilker and Lippard have employed the anionic tetrathiolate $[Zn(SPh)_4]^{2-}$ as a functional model for Ada.[7] They found a methylation of the complex by $(MeO)_3PO$ to yield PhSMe and postulated a dissociative reaction mechanism. Vahrenkamp et al. have studied the methylation of [tris(pyrazolyl)borato]zinc thiolates ($Tp^{R,R}ZnSR$) and have provided strong evidence (gained from kinetic measurements) that these reactions occur intramolecularly and feature a four-center transition structure.[8–10] A similar interpretation has been provided by Carrano et al., who have investigated the methylation of a series of (scorpionato)zinc thiolates.[11–13] Darensbourg et al. have investigated the alkylation of a zinc complex with a bis(thiolate) $[N_2S_2]^{2-}$ chelate ligand.[14] They also obtained the thioether derivatives, but did not discuss the mechanism.

The above (incomplete and arbitrary) list of examples provides insight into some established applications of zinc thiolate complexes as enzyme models. They also resemble, however, the catalytic domain of another important class of enzymes, the matrix metalloproteases (MMPs or matrixins). These play an important role in the degradation of extracellular matrix components, such as collagen.[15,16] The enzymes are secreted into the extracellular space in a latent (inactive) form, the so-called proMMPs, therefore an additional activation step is required to induce protease activity. This is a sensitive process, since the active form can digest its own framework and thus the timing of activation is critical. Furthermore, an imbalance of the active enzyme and its inhibited form is implicated in the pathology of diseases such as arthritis, cancer, multiple sclerosis, and cardiovascular diseases.[17] Thus, it is vitally important to gain a detailed understanding of the activation mechanism.[18]

The catalytic zinc(II) ion in the latent enzymes − the MMP precursor proteins (proMMPs) − is bound to the deprotonated sulfhydryl group of a cysteine and to three histidine residues.[19,20] In vitro experiments have shown that an activation can be achieved with a variety of reagents, but the initial step is always a hydrolytic cleavage of the zinc–sulfur linkage.[21] The coordination sphere of the zinc ion is then completed by a water molecule to form the catalytically active His_3ZnOH motif.[22] A model reaction for this

[a] Institut für Organische Chemie und Makromolekulare Chemie, Humboldtstr. 10, 07743 Jena, Germany
E-mail: ernst.anders@uni-jena.de
[b] Institut für Anorganische und Analytische Chemie, Lessingstr. 8, 07743 Jena, Germany.

process has been reported by Parkin et al., who performed the hydrolytic cleavage of a tripodal S_3Zn–SR complex and obtained free thiolate.[23] To the best of our knowledge, no model complex that resembles the His_3Zn–Cys coordination motif of the inactive enzyme has been used for these investigations so far. Our complexes might thus prove to be useful in this field of research.

Furthermore, recent investigations have suggested that carbonic anhydrase[24,25] plays a pivotal role in the fixation of carbonyl sulfide according to the equation $L_nZnOH + COS \rightarrow L_nZnSH + CO_2$.[26] Quantum mechanical calculations have revealed that a zinc hydrosulfide moiety His_3Zn–SH is formed in the course of this interconversion.[27] A suitable structural model − the neutral hydrosulfide complex $Tp^{Ph,Me}ZnSH$ − has been found by Vahrenkamp et al.[28,29] Our efforts to obtain an equivalent zinc hydrosulfide complex with an azamacrocyclic ligand were not successful because these compounds are not stable. Nevertheless, due to their positive overall charge, our thiolate complexes also could be regarded as suitable model systems for this species.

In this article we focus on the solid-state structures of cationic zinc monothiolates bearing a polyazamacrocyclic ligand. Azamacrocyclic ligands are available with many ring sizes and different numbers of donor atoms, therefore they allow a wide range of complexes to be synthesized with different electronic properties and steric demands. Thus, one can study the influence of the "protein-imitating" ligand on the binding mode and reactivity of a zinc-bound thiolate in great detail. With regard to future investigations or possible synthetic applications, it is convenient to choose the most suitable thiolate complex out of a large pool of substances with different reactivities and solubilities. We cover complexes formed with a wide range of azamacrocycles and reveal insights into both zinc thiolate coordination chemistry and coordination geometries of polyazamacrocyclic ligands on zinc centers. In subsequent articles, we will report on the reactions that these thiolates are capable of undergoing.

Results and Discussion

Starting Materials

Figure 1 illustrates the macrocyclic ligands that we used for complexation experiments. They feature ring sizes varying from 9 to 16 atoms and contain three, four, or five nitrogen donors. In addition, we report the synthesis of a new azamacrocycle, 8-methyl-[11]aneN$_3$ (**4**). All azamacrocycles were prepared using a slightly modified Richman–Atkins procedure.[30]

Complexation Experiments

Zinc monothiolates with macrocyclic amine ligands are a novel class of compounds, and only two such examples are documented in the literature. Koike, Kimura et al.[31] postulated the formation of a complex of $[Zn(cyclen)]^{2+}$ with captopril, a hypertensive drug containing a thiolate function, but they did not characterize this substance. Their work illustrates, however, the biological significance of this type of compounds. In addition, Addison and Sinn have reported the complex *trans*-$[Zn(cyclam)(SC_6F_5)_2]$, which bears two pentafluorothiophenolate ligands.[32] Initially, we prepared our complexes in a similar way by treating equimolar amounts of the macrocyclic ligand with zinc perchlorate in methanol. This was followed by addition of an equimolar amount of sodium thiolate in methanol. The desired compounds $[Zn(L_n)(SR)]ClO_4$ precipitated with good yields. The reaction mode is outlined in Equation (1).

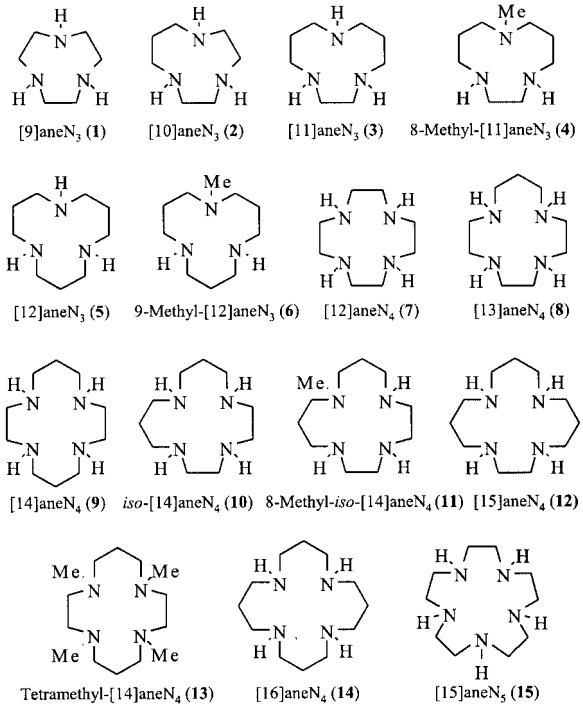

Figure 1. Macrocyclic polyamine ligands used for complexation experiments.

$$L_n + Zn(ClO_4)_2 + NaSR \rightarrow [Zn(L_n)(SR)]ClO_4 + NaClO_4 \quad (1)$$

A higher purity and better yields were achieved with potassium thiolates since the precipitation of potassium perchlorate forces the equilibrium towards the desired products.

However, this synthesis has its limits. The nature of the thiolate has a marked influence on this reaction: only arene- and phenylmethanethiolates yield the desired thiolate complexes. This is in contrast to the [tris(pyrazolyl)borato]zinc thiolates, for which aryl- *and* alkyl derivatives are available.[9] Alkyl thiolates (e.g. MeSH, EtSH, *t*BuSH) only afford the zinc bis(thiolates) $Zn(SR)_2$ and the bis(perchlorate) complexes $[Zn(L_n)](ClO_4)_2$.

Restrictions are also encountered when the ligand does not possess the proper ring size and the right type and number of nitrogen donor sites. If the macrocycle is smaller than 11 atoms (ligands **1** and **2**), the synthesis again yields only the bis(thiolate) salts $Zn(SR)_2$ and complexes of the

composition $[Zn(L_3)_2](ClO_4)_2$. The reason is that small ring systems form extremely stable metal complexes[33] that are much more stable than complexes with larger rings.[34] In addition, 9- and 10-membered cyclic triamines do not react according to a 1:1 stoichiometry with zinc ions, which prevents the coordination of an additional monodentate ligand. Instead, a 1:2 complex precipitates from solutions, thus leaving behind noncomplexed zinc(II), which then forms a bis(thiolate) salt. A similar observation was made in the case of L_4 (tetramethylcyclam, **13**). This ligand always exhibits an unfavorable steric arrangement in its complexes with zinc as well as with other metal ions [it normally adopts the (+ + + +) configuration;[35] see below for details]. These complexes are generally less stable than complexes of its unsubstituted analogue, cyclam (**8**).[36] In the present case, the zinc(II) ion is removed from the macrocycle by formation of the more stable bis(thiolate) of zinc, releasing the free ligand.

Structures

As already mentioned, of all the mercaptans tested only phenylmethane- and arenethiols form the desired complexes. Therefore we synthesized two series of isomeric complexes $[Zn(L_n)(SR)]ClO_4$ employing phenylmethanethiol (**a**; R = $CH_2C_6H_5$) and 4-methylbenzenethiol (**b**; R = $C_6H_4CH_3$). Twenty four novel thiolate complexes were obtained, of which 20 were characterized by single-crystal X-ray diffraction. (In the structure representations, the hydrogen atoms on carbon atoms and the perchlorate ions have been omitted for clarity.)

[Zn(3)(SR)]ClO$_4$ (17) and [Zn(4)(SR)]ClO$_4$ (18)

The complexes derived from the 11-membered ring ligands **3** and **4** are remarkably similar regarding their individual structural parameters. The N_3ZnS unit exhibits a slightly distorted tetrahedral coordination geometry (Figure 2), and all four Zn–S bond lengths are in the very narrow range of 2.2295(5)–2.2394(6) Å. The Zn–N bonds have distances between 2.037(2) and 2.076(2) Å. There is no significant correlation with the nature of the N donor, i.e. secondary or tertiary. The IR spectra show a single N–H band

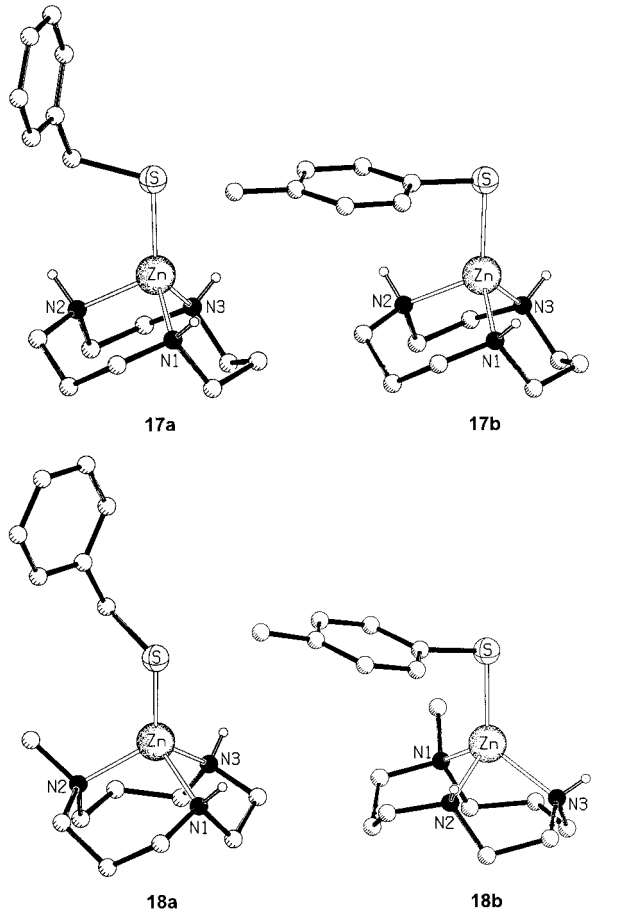

Figure 2. Molecular structures of **17a**, **17b**, **18a**, and **18b**. Selected bond lengths [Å]: **17a**: Zn–S 2.2353(9), Zn–N1 2.044(3), Zn–N2 2.047(3), Zn–N3 2.073(7); **17b**: Zn–S 2.2394(6), Zn–N1 2.056(2), Zn–N2 2.066(4), Zn–N3 2.048(2); **18a**: Zn–S 2.2295(5), Zn–N1 2.076(2), Zn–N2 2.060(2), Zn–N3 2.066(2); **18b**: Zn–S 2.2358(5), Zn–N1 2.068(2), Zn–N2 2.065(2), Zn–N3 2.037(2).

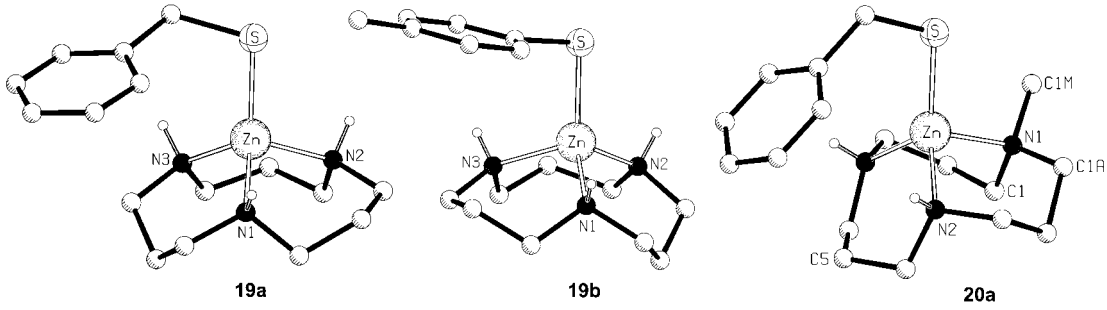

Figure 3. Molecular structures of **19a**, **19b**, and **20a**. Selected bond lengths [Å]: **19a**: Zn–S 2.245(2), Zn–N1 2.046(3), Zn–N2 2.056(3), Zn–N3 2.052(3); **19b**: Zn–S 2.2492(9), Zn–N1 2.036(3), Zn–N2 2.032(3), Zn–N3 2.052(3); **20a**: Zn–S 2.2367(7), Zn–N1 2.075(2), Zn–N2 2.050(2).

in the range of 3261–3271 cm^{-1}, which is broadened to a varying extent. This indicates the high degree of chemical analogy of these hydrogen atoms. Interestingly, the ligand's methyl substitution in **18a** has a marked effect on its solubility; it is readily soluble in dichloromethane, while the unsubstituted analogue, **17a**, is not.

[Zn(5)(SR)]ClO_4 (19) and [Zn(6)(SR)]ClO_4 (20)

The three structurally characterized compounds **19a**, **19b**, and **20a** (Figure 3), synthesized with ligands **5** and **6**, show the same geometrical equivalence as observed for the complexes **17** and **18**. Slightly longer Zn–S bonds than in the case of the 11-membered cycles are encountered. However, the values for the Zn–N bonds are found in the same range. The IR spectra again show single bands in the region between 3252 and 3259 cm^{-1}. If the complex is asymmetric, they are broadened as mentioned above. Compound **20a** is symmetric along the C5–Zn–S plane (apart from a disorder of the atoms C1, C1A, N1, and C1M); therefore, the two hydrogen atoms attached to N2 and N2A are identical and give rise to a single, very narrow IR absorption. This shows the usefulness of IR absorption bands of N–H groups in determining the symmetry properties of macrocyclic amine complexes, a concept which will be referred to again later. Complex **20b** also exhibits a single band at almost the same value as **20a**, but it is noticeably broadened. This indicates the absence of a strict symmetry here. However, the structure is likely to follow the same motif. Similar to **18a**, the additional methyl group induces a solubility of **20a** in dichloromethane.

Coordination Geometries in N_4 Complexes

Whether a five-coordinate complex belongs to the trigonal-bipyramidal or the tetragonal-pyramidal type is a question which is tricky to answer in the present case. Justifying an answer solely by the values of the bond angles, and thus seeking a more or less distorted trigonal bipyramidal axis, does not suffice. Upon first inspection, all the structures would appear to be a form of distorted square pyramid (see Figures 4–7 below). One thus needs to pay closer attention to the Zn–N bond lengths. In some cases (**23a**, **23b**, and to a lesser extent **27a**), the Zn–N bonds have almost the same lengths and the coordination polyhedra should therefore be regarded as being tetragonal-pyramidal with the sulfur atom in the apical position. The other complexes exhibit strongly differing values for pairs of opposing Zn–N bonds. They can therefore be classified as trigonal-bipyramidal. In these cases the thiolate ligand assumes an equatorial position. This effect is most strongly pronounced in complex **26a** (Figure 7): the mean deviation between adjacent Zn–N bond lengths is nearly twice as large (0.14 Å) as the difference between the *average* Zn–N and Zn–S bond length (0.08 Å). The species **21a** and **21b** must be classified as being "in between", since they exhibit neither a peculiar "axis" nor sufficiently small deviations in the Zn–N bond lengths.

The nitrogen atoms in these complexes are chiral in nature and we describe their actual configuration using established conventions.[37,38] The positions of hydrogen atoms or methyl groups are denoted relative to a plane (or near-plane) defined by the nitrogen atoms. If the N-bound residues are found on the side of the complex that bears the thiolate, their position is indicated with a (+). N-bound residues opposite the thiolate side are denoted with a (–). It is obvious that the configuration of the N_3 complexes is always (+ + +), as is expected for ligands whose cavities are too small for the respective metal ion.[37]

[Zn(7)(SR)]ClO_4 (21) and [Zn(8)(SR)]ClO_4 (22)

The ring size of ligands **7** and **8** is rather small and all four structures accordingly exhibit the (+ + + +) configuration (Figure 4). Although compounds **21** both have a pair of opposing "long" and "short" bonds, the difference of both "axes" is too small to consider the geometries as being

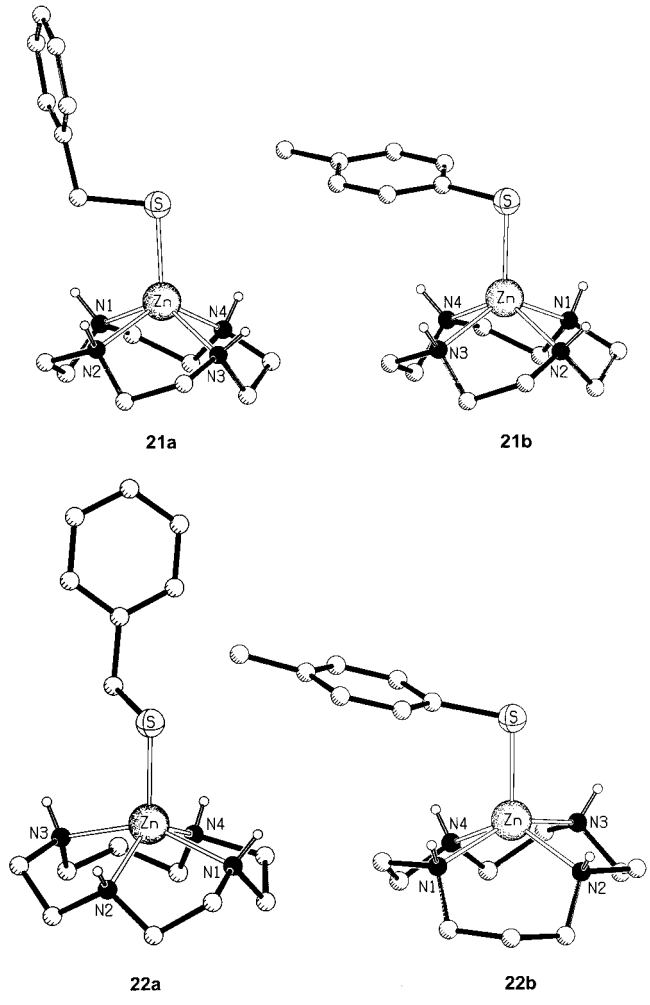

Figure 4. Molecular structures of **21a**, **21b**, **22a**, and **22b**. Selected bond lengths [Å]: **21a**: Zn–S 2.266(2), Zn–N1 2.159(4), Zn–N2 2.205(5), Zn–N3 2.151(4), Zn–N4 2.176(4); **21b**: Zn–S 2.2796(7), Zn–N1 2.175(2), Zn–N2 2.143(3), Zn–N3 2.201(3), Zn–N4 2.162(2); **22a**: Zn–S 2.2853(9), Zn–N1 2.218(3), Zn–N2 2.127(3), Zn–N3 2.187(3), Zn–N4 2.114(4); **22b**: Zn–S 2.2957(5), Zn–N1 2.200(2), Zn–N2 2.109(2), Zn–N3 2.208(2), Zn–N4 2.138(2).

trigonal-bipyramidal. The reason for this distortion is the small ring size of the ligand **7**, which enforces a marked rigidity in the coordination polyhedron. Although the system obviously strives for bipyramidality, steric constraints imposed by the ring force a tetragonal-pyramidal structure. In the case of complexes **22**, the ring is considerably larger and allows the formation of a (severely distorted) trigonal bipyramid. In agreement with this assignment, the IR spectra show a single N–H stretching band for complexes **21a** (3292 cm^{-1}) and **21b** (3301 cm^{-1}), emphasizing the degree of equivalence of the nitrogen atoms. In contrast to this, the N–H protons of compounds **22** are chemically inequivalent and three stretching bands are observed for both **22a** (3276, 3288, and 3306 cm^{-1}) and **22b** (3272, 3289, and 3322 cm^{-1}).

[Zn(9)(SR)]ClO$_4$ (23)

With regard to the other [N_4] ligands, cyclam (**9**) yields an unusual result as complexes of **9** are the only ones which exhibit an almost perfect square-pyramidal geometry (Figure 5). This is particularly surprising since the ligand is clearly large enough to allow the formation of a trigonal bipyramid. The influence of the thiolate ligand on the conformation is minimal. All the Zn–N bond lengths are almost identical, with their maximum deviation being less than 0.02 Å for **23a** and 0.01 Å for **23b**. The two Zn–S bond lengths are identical within experimental error. Both complexes exhibit a (+ + – –) configuration which has been reported as being generally the most stable geometry.[39] Of the investigated complexes, **23b** is the only one which possesses a rigorous molecular symmetry (C_s) in the solid state, with the plane of symmetry being defined by C1, Zn, and S. The IR spectrum of **23b** thus exhibits two extraordinarily sharp N–H stretching bands at 3270 and 3259 cm^{-1} with exactly the same intensity. In contrast, the absorptions of **23a** at 3272 and 3259 cm^{-1} are not as sharp and their intensities show a marked difference.

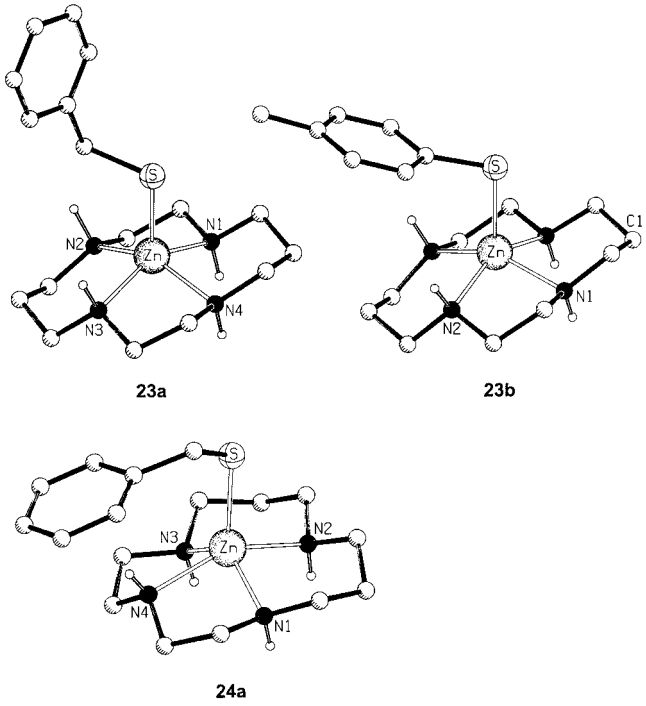

Figure 5. Molecular structures of **23a**, **23b**, and **24a**. Selected bond lengths [Å]: **23a**: Zn–S 2.3161(7), Zn–N1 2.155(2), Zn–N2 2.151(2), Zn–N3 2.149(2), Zn–N4 2.139(2); **23b**: Zn–S 2.3174(8), Zn–N1 2.139(2), Zn–N2 2.147(2); **24a**: Zn–S 2.2902(6), Zn–N1 2.112(2), Zn–N2 2.187(2), Zn–N3 2.123(2), Zn–N4 2.218(2).

[Zn(10)(SR)]ClO$_4$ (24)

Complex **24a** possesses a (+ – – –) configuration which complies with the structural symmetry of the ligand (Figure 5). The symmetry of **24a** results in essentially two amine bands in its IR spectrum. One is located at 3268 cm^{-1} (br., N1–H, N2–H, N3–H) and apparently consists of two closely overlapping bands, and the second band at 3309 cm^{-1} is quite sharp (N4–H). The IR spectrum of **24b** is very similar. It also exhibits two bands at 3248 and 3305 cm^{-1}. We therefore assume that **24b** is very likely to have the same configuration.

[Zn(11)(SR)]ClO$_4$ (25)

The most significant difference between the two compounds derived from ligand **11** is the configuration of the tertiary nitrogen atom, which is found to be (+) in complex **25a** and (–) in **25b**. This results in differing symmetries for the complexes (Figure 6). A related observation has been reported by Alcock et al.,[40] who have determined from ^{1}H NMR spectroscopic data that a D_2O solution of [Zn(**11**)]$(NO_3)_2$ contains two isomers, one of which is symmetric and the other asymmetric. In the present case, this effect can be observed in the ^{1}H NMR spectrum of **25a** but not for **25b** due to the lack of an isolated signal. The benzylic methylene protons of **25a** yield two peaks at δ = 3.80 and 3.76 ppm with a relative intensity of 5:1. Its ^{13}C NMR spectrum shows a predominant set of signals with five ring methylene peaks. For **25b**, two different ^{13}C NMR spectroscopic data sets could be detected for the methylene carbon atoms of the macrocycle, a major set with five peaks and a

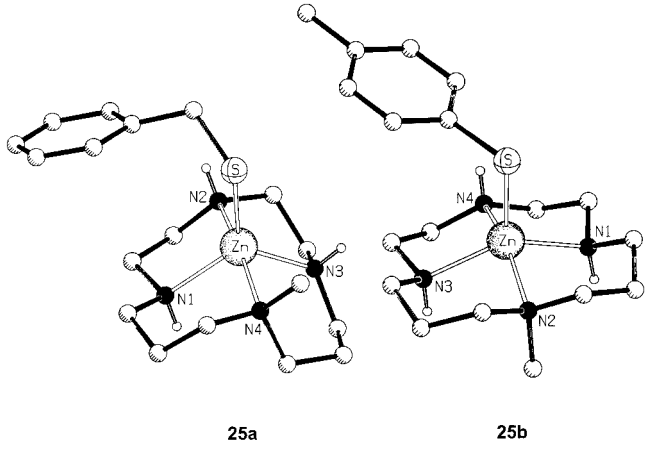

Figure 6. Molecular structures of **25a** and **25b**. Selected bond lengths [Å] and angles [°]: **25a**: Zn–S 2.3200(7), Zn–N1 2.118(2), Zn–N2 2.235(2), Zn–N3 2.133(2), Zn–N4 2.202(2); N2–Zn–N4 165.81(9); **25b**: Zn–S 2.3182(9), Zn–N1 2.106(3), Zn–N2 2.171(3), Zn–N3 2.105(3), Zn–N4 2.191(3); N2–Zn–N4 154.3(2).

minor set consisting of ten peaks. We thus assume that in both cases the predominant species is of the same symmetric configuration as found in the solid-state structure of **25b**. The minor component is of an asymmetric configuration, analogous to the solid-state structure of **25a**.

The fact that the crystal lattices of **25a** and **25b** contain different configurational isomers is also reflected in their IR spectra. Three N–H bands at 3239, 3308 and 3346 cm^{-1} are present in the case of the unsymmetrically configured **25a** and only two at 3246 (br.) and 3293 cm^{-1} for the symmetric ligand configuration found in **25b**.

[Zn(12)(SR)]ClO_4 (26)

As mentioned above, **26a** (synthesized from ligand **12**) has the largest deviations in its Zn–N bond lengths. It clearly adopts a trigonal-bipyramidal geometry and a (+ – – –) configuration of the nitrogen atoms (denoted in the order N1–N2–N3–N4; see Figure 7). Similar to **25a**, the NMR spectra reveal that a chloroform solution of complex **26a** contains two isomers. The ^{13}C NMR spectrum exhibits 11 methylene carbon peaks for the main component and seven for the minor component. The major component possesses an asymmetric configuration of the chiral nitrogen atoms, which is very likely identical to the solid-state structure of this compound. The symmetric configuration of the minor component might be (+ – – +) or all-(–), but this question could not be answered from the routine NMR spectroscopic data. The ^1H NMR spectrum shows a multiplet for the benzylic methylene protons. Upon closer inspection, this multiplet consists of a singlet at δ = 3.85 ppm (minor component, 15% of total integral value of benzyl protons) overlapping with an AB spin system at δ = 3.81 ppm (main component, J = 14.3 Hz, $\Delta\delta$ = 9.7 Hz). This observation fits perfectly, since the asymmetric configuration of the nitrogen atoms ensures a chiral zinc atom. The benzyl protons are thus in a diastereotopic environment, which causes the multiplicity of their NMR signal. (Why this is only observed for **25a** and not for the other complexes of asymmetric configuration remains a mystery. A possible explanation could be found in different velocities of configurational change, which might cause enhanced line-widths for the other complexes and render the detection of signal multiplicities impossible. However, we are not sure about this.) The IR spectrum shows only three bands at 3251, 3266, and 3286 cm^{-1}, which is not surprising since the structural environments of N2 and N4 are very similar. For compound **26b**, only one structural motif could be obtained by X-ray crystallography. It reveals, however, that the configuration of the ligand is the same as found in **26a**.

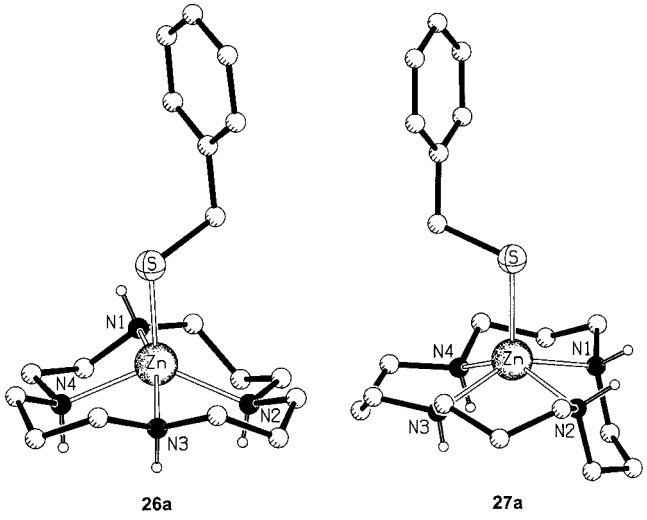

Figure 7. Molecular structures of **26a** and **27a**. Selected bond lengths [Å]: **26a**: Zn–S 2.28(2), Zn–N1 2.271(3), Zn–N2 2.115(3), Zn–N3 2.256(3), Zn–N4 2.123(3); **27a**: Zn–S 2.299(2), Zn–N1 2.208(3), Zn–N2 2.182(3), Zn–N3 2.194(3), Zn–N4 2.189(3).

[Zn(14)(SR)]ClO_4 (27)

Ligand **14** is known to form complexes that are less stable than complexes formed from smaller macrocycles. A detailed study has shown that the steric strain in the six-membered chelate rings is responsible for this.[37] Zinc(II) tends to form the complex [Zn(**14**)]$(ClO_4)_2$ with a (+ – + –) configuration. Its stability stems from the fact that the metal ion's size and the Zn–N bond length ensure a chair conformation in each of the four chelate rings. A mixture of this compound with **27a** was obtained when sodium thiolate was used for synthesis; only the potassium salt afforded the pure thiolate complex. In the case of **27a**, the central Zn^{2+} ion is pentacoordinate (Figure 7), which obviously does not allow the nitrogen atoms to arrange in a tetrahedral manner. However, the ligand folds in such a way that only chelate rings with a chair conformation are formed. The N–Zn–N angles of the adjacent nitrogen atoms vary between 78 and 89°. Obviously, ring strain is low enough to render the complex more stable than [Zn(**14**)]$(ClO_4)_2$. In accordance with the observed molecular symmetry, the IR spectrum of **27a** shows only one N–H absorption at 3249 cm^{-1}. Two IR bands were observed for compound **27b**, which comply with two pairs of chemically nonequivalent hydrogen atoms. This does not, however, necessarily indicate the presence of another configuration.

[Zn(15)(SR)]ClO_4 (28)

When sodium thiolate was used to synthesize complex **28a**, the sulfur-free complex [Zn(**15**)]$(ClO_4)_2$ (**16**) was obtained instead (Figure 8). Only the use of the potassium salt afforded complex **28a**, while **28b** was also obtained with sodium *p*-methylbenzenethiolate. These compounds and complex **16** are the first reported zinc complexes of the ligand [15]aneN_5 (**15**). They all show a high degree of structural equivalence regarding the configuration of the macrocycle. The unit cell of **28b** contains two independent molecules with almost superimposable coordination polyhedra, although noticeable deviations in the bond lengths are encountered. Since the two molecules have nearly the same appearance, only one of them is depicted in Figure 8.

These hexacoordinate zinc complexes with the rare N_5S coordination environment (only one structurally charac-

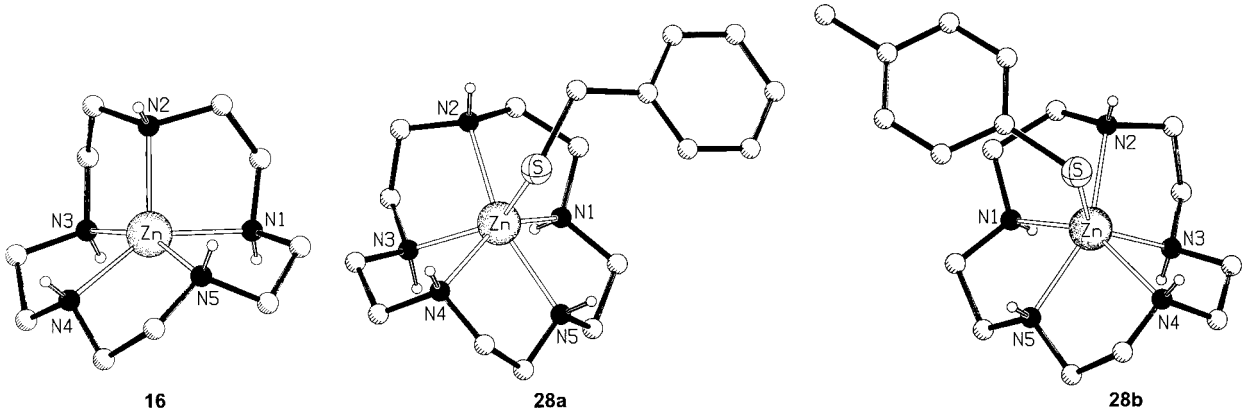

Figure 8. Molecular structures of **16**, **28a**, and **28b**. Selected bond lengths [Å]: **16**: Zn–N1 2.100(2), Zn–N2 2.067(2), Zn–N3 2.170(2), Zn–N4 2.179(2), Zn–N5 2.168(2); **28a**: Zn–S 2.3782(7), Zn–N1 2.199(3), Zn–N2 2.366(3), Zn–N3 2.192(3), Zn–N4 2.368(3), Zn–N5 2.221(3); **28b** (molecule A): Zn–S 2.405(2), Zn–N1 2.206(7), Zn–N2 2.331(6), Zn–N3 2.152(5), Zn–N4 2.385(6), Zn–N5 2.194(5); (molecule B, not depicted): Zn–S 2.435(2), Zn–N1 2.265(5), Zn–N2 2.309(6), Zn–N3 2.199(5), Zn–N4 2.307(6), Zn–N5 2.205(5).

terized example has been reported until now[41]) do not have much in common with the other complexes discussed in this work. Their coordination polyhedra cannot be assigned to a specific structure type. Of the complexes discussed in this study, **28a** reveals the largest mean Zn–N bond length (2.267 Å), and **28b** shows the largest deviation within a single molecule (0.23 Å). However, the most significant characteristics are probably the zinc–sulfur bond lengths, which are 2.3782(7) Å for **28a** and 2.405(2) and 2.435(2) Å for **28b**, respectively. These are extraordinarily long Zn–S bonds compared to the average bond length of 2.29 Å for terminal zinc thiolates listed in the Cambridge Structural Database.[1] This makes complexes **28** somewhat equivalent to the zinc tetrathiolate *anion* $[Zn(SPh)_4]^{2-}$, which has a Zn–SPh bond length of 2.36 Å,[42,43] and accentuates their exceptional structural properties.

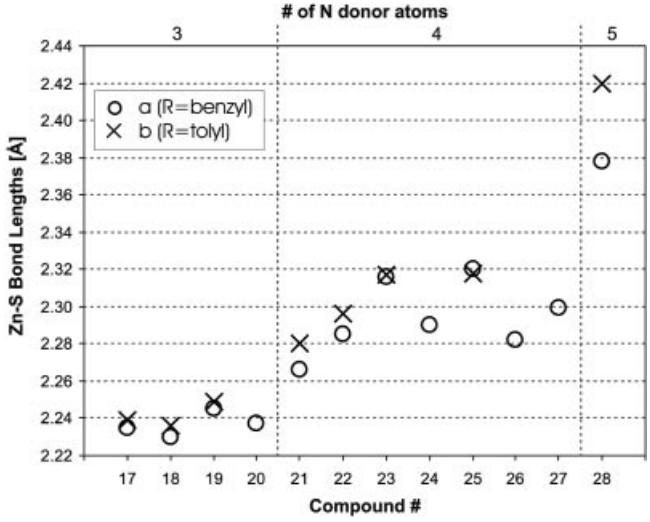

Figure 9. Zn–S bond lengths [Å] (mean value for **28b**).

Comparative Considerations

Figure 9 shows that the Zn–S bond lengths depend on the number or the nature of the nitrogen donor sites in only a loose way. It is much more obvious that there is a certain correlation with the ring size: as it increases from 11 to 13 atoms, the Zn–S bond lengths increase from approx. 2.23 to 2.29 Å. The Zn–S bonds in complexes with 14-membered or larger rings (compounds **23** to **27**) seem to scatter around a "standard" length of approx. 2.3 Å, which is close to the average zinc thiolate linkage of 2.29 Å as mentioned above. The fact that compounds **28** are much less stable than the other complexes is reflected in their extremely long Zn–S bonds.

In contrast to the previous case, it is not the ring size of the macrocyclic ligand but rather the number of nitrogen donors that seems to have the pivotal influence on the average Zn–N bond lengths. The plot depicted in Figure 10 reveals three distinct groups of compounds, corresponding to the number of nitrogen atoms involved. Their secondary or tertiary nature does not contribute to a Zn–N bond length alteration in a noticeable way. As far as can be

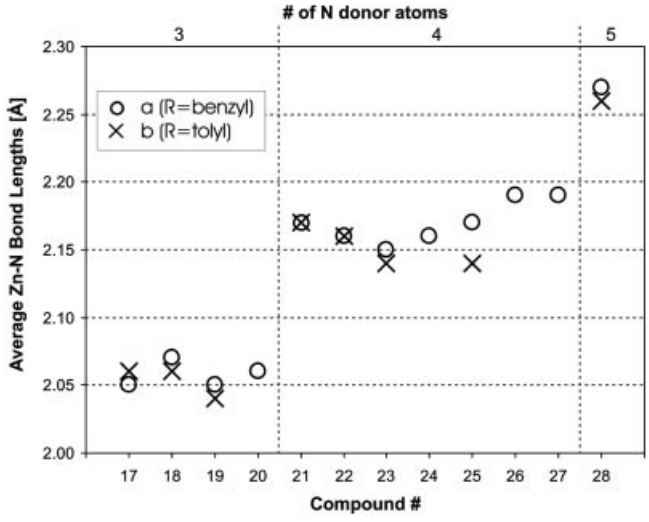

Figure 10. Average Zn–N bond lengths [Å].

judged from this incomplete data (four structures are missing), the type of thiolate has no significant influence either.

NMR Spectra

The ^{1}H NMR spectra generally show only nonspecific multiplets and broadened peaks for the hydrogen atoms attached to the macrocycle. This is very likely caused by dynamic effects. Measurements of gradually diluted solutions with concentrations ranging from 0.1 to 4 mM yield unaltered spectra. This allows the conclusion that there is no distinct contribution of intermolecular interactions. Only the benzyl methylene, the tolyl methyl groups, and the aromatic hydrogen atoms exhibit the usual line shape. However, their shifts show only very little dependence on macrocycle substitution. Nevertheless, these signals are suitable for reaction monitoring.

The ^{13}C NMR spectra are resolved much better, even though they sometimes exhibit considerably increased linewidths for the methylene carbon atoms of the macrocyclic ligands. For all complexes but **26**, the number of detected methylene peaks is smaller than the number of methylene carbon atoms of the macrocycle and correlates directly with the valence symmetry of the macrocyclic ligand. This allows the conclusion that either the complexes adopt a symmetrical structure in solution or the dynamic conformational changes proceed quickly enough to override the asymmetry of the macrocycle that originates in the conformation enforced by the metal coordination. Nevertheless, compounds **19**, **20b**, **22**, **23a**, **25b**, and **26** exhibit additional signals of small intensities for the carbon atoms of the macrocycle. This indicates the presence of at least one additional isomer. In case of the more rigid systems **19**, **20b**, and **22** it is possible that conformational changes in the bridging ethylene and propylene units require comparably high energy barriers and hence are slow on the NMR timescale, thus allowing the detection of the conformers as separate signal sets. Another possible interconversion between species in solution is the configuration inversion of a chiral nitrogen atom. This seems to hold for **23a**, **26**, and particularly for **25b** (see discussion of structures above).

Mass Spectra

Mass spectra, recorded in ESI mode with a mixture of MeOH and MeCN as solvents, provide valuable information on the stability of the Zn–S bond. The weaker the thiolate is bound, the more species are detected with the monodentate thiolate ligand being replaced by HO^-, MeO^-, or MeCN, or simply without the ligand. Thus, the intensity of these signals as compared to the molecular peak $[Zn(L_n)(SR)]^+$ may be considered as an indicator of complex stability.

According to this approach, the mass spectra reveal the complexes containing small macrocyclic ligands to be the most stable. All complexes with rings of up to 12 atoms (**17**–**21**) show none or only small amounts (up to 10% intensity) of the mentioned degradation products. For the compounds with 13- to 16-membered rings (**28** not considered), the peak intensities of the solvent complexes increase with the ring size, reaching a maximum for compounds **27**. In addition, the aromatic thiolate yields complexes of considerably higher stability than phenylmethanethiolate. This agrees with the observations made during the preparation of **27a** and **28a**. The "overcrowded" complexes **28** are the least stable ones. In the case of the phenylmethanethiolate complex **28a**, the molecular peak could not even be detected. In no case was any evidence for a dissociation of the macrocycle from the zinc center found.

Conclusions

Azamacrocycles have been found to be suitable ligands to obtain stable, soluble thiolate complexes of Zn^{II}. In retrospect, this cannot be taken as a matter of course. The fact that only certain ring sizes and thiolates yield the desired complexes illustrates how sensitive these systems are to steric and electronic influences. (It is worth mentioning that substituted arene- and phenylmethanethiolates are generally suitable for these syntheses, as some additional experiments have shown. However, a more detailed investigation of the issue has not been performed because we did not expect it to provide any fundamentally enhanced insight into the matter.) It is surprising that the crystal lattices of all complexes comprise only monomeric structures. We assume that the steric demand of the benzyl and aryl residues of the thiolate ligands is a substantial factor behind this behavior. Less sterically hindered thiolates such as MeS^- would presumably promote the formation of dimers or oligomers. However, this will probably remain speculation because these compounds are elusive and our efforts to develop alternative synthetic routes were not successful.

The main advantage of this class of complexes is its structural diversity. A large number of thiolate–zinc linkages that differ in length, stability, and bond order can be studied. With the exception of **28**, their solubility in non- and semipolar organic solvents allows the investigation of reactions under conditions that resemble the hydrophobic cavities of enzyme proteins. In addition, there are two characteristics that make them ideally suited for studies combining experimental work and computational methods. First, their molecular structure data are, except for a few examples, available with high accuracy. Second, they contain a comparably small number of non-hydrogen atoms. Thus, quantum mechanical calculations of these compounds can actually be performed at sufficiently high levels of theory to gain insight into reaction mechanisms. Finally, their easy accessibility, long-term stability, and the variety of characterized compounds renders this class of complexes useful for biomimetic studies wherever zinc thiolates are involved.

Experimental Section

Materials and Methods: All reagents used were of analytical purity. Solvents were not dried prior to use, except where indicated. NMR

spectra were recorded using a Bruker AC 250 spectrometer at a temperature of 30 °C. IR spectra were recorded from the neat substances using a Nicolet Avatar 320 FT-IR spectrometer. Elemental analyses were performed using a Heraeus Vario EL III system. Melting points were determined with a Büchi Melting Point B 545 apparatus and are uncorrected. Mass spectra were recorded using a Finnigan MAT SSQ 710 or a Finnigan MAT 900XL TRAP.

Preparation of the Azamacrocycles: The preparation essentially followed a published procedure.[30] Small alterations were made to the reaction conditions of the cyclization (2–3 h at 125 °C) and the workup procedure of the deprotected amine. The preparation of 8-methyl-[11]aneN_3 (**4**) serves as an example.

Preparation of 8-Methyl-1,4,8-triazacycloundecane (8-Methyl-[11]aneN_3) (4): A solution of the disodium salt[30] of *N*,*N*-bis[3-(*p*-tolylsulfonyl)aminopropyl]methylamine[44] (88 mmol) and 1,2-bis(*p*-tolylsulfonyloxy)ethane (88 mmol) in dry DMF (1.5 L) was stirred at 140 °C for 3 h. Three-quarters of the solvent was then distilled off in vacuo and the mixture was poured into 1 L of an ice/water mixture. The product was filtered off, washed with plenty of water, and recrystallized from ethanol to yield 56% of 8-methyl-1,4-bis(*p*-toluenesulfonyl)-1,4,8-triazacycloundecane as a colorless solid. M.p. 161 °C. ^{1}H NMR (250 MHz, $CDCl_3$): δ = 1.78 (q, J = 5.65 Hz, 4 H, CH_2), 2.19 (s, 3 H, N–CH_3), 2.45 (s, 6 H, Ph–CH_3), 2.58 (t, J = 6.25 Hz, 4 H, CH_2), 3.16 (t, J = 5.73 Hz, 4 H, CH_2), 3.37 (s, 4 H, CH_2), 7.30 and 7.69 (d, J = 6.56 Hz, 4 H each, Ph–*H*) ppm. ^{13}C NMR (62.9 MHz, $CDCl_3$): δ = 21.5, 24.4, 42.4, 48.5, 50.8, 52.5, 127.5, 129.7, 134.9, 143.4 ppm. $C_{23}H_{33}N_3S_2O_4$ (479.67): calcd. C 57.59, H 6.39, N 8.76, S 13.37; found C 57.32, H 7.17, N 8.60, S 13.24. For detosylation, the solid was heated in concd.

Table 1. Analytical data for compounds **17**–**28**.

Complex	Composition calcd. [%]					Complex	Composition found [%]					Yield	M.p.[a]
	C	H	Cl	N	S		C	H	Cl	N	S	[%]	[°C]
17	40.46	5.98	7.96	9.44	7.20	**17a**	40.47	6.24	8.00	9.48	6.95	37	228–230
						17b	40.31	5.86	7.82	9.36	6.72	53	310 d
18, **19**	41.84	6.14	7.72	9.15	6.98	**18a**	41.78	6.19	7.94	9.09	6.55	53	162–164
						18b	41.77	6.16	7.99	9.09	6.53	21	228–229
						19a	41.67	6.17	7.83	9.02	6.50	46	187–190
						19b	41.75	6.05	7.54	9.07	6.61	65	309 d
20	43.39	6.39	7.49	8.87	6.77	**20a**	43.03	6.45	7.30	8.82	6.51	53	158–160
						20b	43.00	6.33	7.69	8.78	6.32	49	218–220
21	39.41	5.91	7.70	12.17	6.97	**21a**	39.01	5.88	7.54	12.10	6.44	35	253–256
						21b	39.05	6.98	7.41	12.16	6.66	73	310d
22	40.52	6.16	7.47	11.81	6.76	**22a**	40.36	6.25	7.50	11.82	6.28	31	216–218
						22b	40.41	6.23	7.51	11.90	6.45	50	292 d
23, **24**	41.81	6.4	7.26	11.47	6.57	**23a**	41.66	6.32	7.01	11.49	6.17	61	204–206
						23b	41.66	6.36	6.99	11.39	6.22	79	276 d
						24a	41.80	6.16	7.05	11.49	6.40	60	221–223
						24b	41.64	6.47	7.01	11.33	6.09	67	275 d
25, **26**	43.03	6.62	7.06	11.15	6.38	**25a**	42.88	6.58	6.88	11.14	6.04	41	211–213
						25b	42.90	6.77	6.96	11.24	6.09	56	230–232
						26a	42.95	7.19	7.40	11.15	6.12	38	193–195
						26b	42.67	6.73	6.77	11.15	5.75	47	272 d
27a	43.80	7.17	6.46	10.21	5.85	**27a**	43.58	7.22	6.58	10.21	5.60	60	173–175
27b	44.19	6.83	6.86	10.84	6.21	**27b**	44.07	6.98	6.96	10.85	6.10	54	270 d
28	40.56	6.41	7.04	13.91	6.37	**28a**	40.21	6.31	7.36	13.97	6.00	20	182–183
						28b	40.48	6.53	7.25	13.92	6.06	66	248 d

[a] d: decomposition.

Table 2. Spectroscopic data for compounds **17**–**28**.

Complex	MS [*m*/*z* (%)][a]	IR [cm^{-1}][b]	Complex	MS [*m*/*z* (%)][a]	IR [cm^{-1}][b]
17a	344 (100)	3271	**23a**	387 (100), 281 (94)	3272, 3259
17b	344 (100)	3246	**23b**	387 (100), 281 (35)	3270, 3259
18a	358 (100)	3268	**24a**	387 (100), 281 (64)	3309, 3268
18b	358 (100)	3261	**24b**	387 (100), 281 (34)	3305, 3248
19a	358 (100)	3254	**25a**	401 (100), 295 (46)	3346, 3308, 3239
19b	358 (100)	3259	**25b**	401 (100), 295 (54)	3293, 3246
20a	372 (100)	3256	**26a**	401[c] (75), 295 (100)	3286, 3266, 3251
20b	372 (100)	3252	**26b**	401 (100), 295 (63)	3275, 3244
21a	359 (100)	3292	**27a**	415[c] (33), 309 (100)	3249, (3199, O–H)
21b	359 (100)	3301	**27b**	415 (100), 309 (87)	3274, 3226
22a	373 (100), 267 (20)	3306, 3288, 3276	**28a**	278 (100),[d] 139 (46)	3353, 3338, 3278
22b	373 (100), 267 (16)	3322, 3289, 3272	**28b**	402[c] (29), 278 (100)	3352, 3329, 3306, 3268

[a] Only the molecular peak and the peak of the main degradation product $[Zn(L)(OH)]^+$ are given. [b] Only the data of the N–H absorptions are denoted. [c] Molecular peak (where different from base peak). [d] No molecular peak detected.

H_2SO_4 (100 mL) for 72 h. A saturated NaOH solution was used to neutralize the H_2SO_4 until a pH of 12 was reached. The amine was extracted with chloroform (5×100 mL), the combined extracts were dried with Na_2SO_4, the solvent was evaporated, and the crude product distilled using a kugelrohr apparatus (b.p. 100 °C, 0.1 mbar) to give 2.75 g (32%) of **4** as a colorless oil. IR: $\tilde{\nu}$ = 3289 m (NH), 2918 s, 2833 (CH_2), 2869 s, 2789 s (CH_3), 1677 m, 1456 s, 1144 s, 1119 s, 1058 s, 737 s cm^{-1}. ^1H NMR (250 MHz, $CDCl_3$): δ = 1.48 (q, J = 5.26 Hz, 4 H, CH_2–CH_2–CH_2), 2.09 (s, 3 H, N–CH_3), 2.42 (t, J = 5.43 Hz, 4 H, MeN–CH_2), 2.63 (s, 4 H, CH_2–CH_2), 2.68 (t, J = 5.29 Hz, 4 H, HN–CH_2) ppm. ^{13}C NMR (62.9 MHz, $CDCl_3$): δ = 25.65, 41.76, 47.43, 48.13, 57.36 ppm. $C_9H_{21}N_3$ (171.26): calcd. C 62.74, H 12.87, N 24.39; found C 59.28, H 12.19, N 22.83 (hygroscopic material; no exact determination of sample weight possible).

Preparation of [Zn([15]aneN$_5$)](ClO$_4$)$_2$ (16): [15]aneN$_5$ (**15**; 1 mmol) was added to a 0.1 M solution of $Zn(ClO_4)_2 \cdot 6H_2O$ (10 mL) in H_2O. After heating for 10 min, the mixture was cooled. A colorless precipitate separated within several hours. The crystals were filtered off, washed twice with ethanol, and dried in vacuo to give 179 mg of **16** (37%) as colorless crystals, m.p. 182–184 °C. $C_{10}H_{25}Cl_2N_5O_8Zn$ (479.36): calcd. C 25.04, H 5.25, Cl 14.78, N 14.60; found C 24.95, H 5.18, Cl 14.60, N 14.65. MS: m/z (%) = 378 (100), 278 (28), 160 (18), 140 (31). ^1H NMR (250 MHz, DMSO): δ = 2.1–2.65 (m, 10 H), 2.65–3.15 (m, 10 H), 3.4–3.9 (br. m, 5 H,

Table 3. ^1H NMR spectroscopic data for compounds **17**–**28** (δ [ppm], 250 MHz, 30 °C). Due to dynamic effects only unspecific multiplets are obtained for the hydrogen atoms of the macrocyclic ligand. Thus, only the data of the protons of the thiolate ligands are given.

Complex	$C_6H_5CH_2$	$C_6H_5CH_2$	Complex	$C_6H_5CH_2$	$C_6H_5CH_2$
17a[a]	3.71 (s)	7.21 (t), 7.33 (t), 7.47 (d)	**17b**[a]	2.25 (s)	6.98 (d), 7.29 (d)
18a[a]	3.70 (s)	7.21 (t), 7.33 (t), 7.43 (d)	**18b**[a]	2.25 (s)	6.98 (d), 7.27 (d)
19a[a]	3.73 (s)	7.22 (t), 7.33 (t), 7.45 (d)	**19b**[a]	2.25 (s)	6.98 (d), 7.31 (d)
20a[a]	3.73 (s)	7.21 (t), 7.34 (t), 7.45 (d)	**20b**[a]	2.25 (s)	6.99 (d), 7.33 (d)
21a[a]	3.65 (s)	7.22 (t), 7.30 (t), 7.43 (d)	**21b**[a]	2.24 (s)	6.94 (d), 7.24 (d)
22a[a]	3.66 (s)	7.19 (t), 7.31 (t), 7.44 (d)	**22b**[a]	2.24 (s)	6.95 (d), 7.26 (d)
23a[b]	3.79 (s)	7.19 (t), 7.31 (t), 7.48 (d)	**23b**[b]	2.26 (s)	6.99 (d), 7.28 (d)
24a[b]	3.73 (s)	7.15 (t), 7.23 (t), 7.41 (d)	**24b**[b]	2.26 (s)	6.95 (d), 7.33 (d)
25a[b]	3.80 (s), 3.76 (s) (20%)[d]	7.17–7.33 (m), 7.40–7.48 (m)	**25b**[b]	2.25 (s)	6.95 (d), 7.29 (d)
26a[b]	3.81,[e] 3.85 (s) (15%)[d]	7.15–7.32 (m), 7.41–7.50 (m)	**26b**[b]	2.26 (s)	6.89–7.43 (m)
27a[b]	3.84 (s)	7.15 (t), 7.22 (t), 7.29 (d)	**27b**[b]	2.25 (s)	6.90 (d), 7.42 (d)
28a[c]	3.57 (s)	7.09 (t), 7.22 (t), 7.29 (d)	**28b**[c]	2.15 (s)	6.82 (d), 7.21 (d)

[a] In CD_3CN. [b] In $CDCl_3$. [c] In [D_6]DMSO. [d] Multiple peaks detected, percentage of minor peak given in brackets. [e] AB spin system, J = 14.3 Hz, $\Delta\delta$ = 9.7 Hz.

Table 4. ^{13}C NMR spectroscopic data (62.3 MHz, 30 °C) for compounds **17**–**28**.

Complex	Solvent	δ [ppm]
17a	CD_3CN	23.5, 28.6, 45.1, 48.3, 126.0, 127.9, 128.3, 146.1
18a	CD_3CN	22.6, 28.6, 45.0, 48.0, 48.2, 58.4, 126.0, 127.9, 128.3, 146.0
19a[a]	CD_3CN	126.0, 127.9, 128.2, 146.0
20a	CD_3CN	23.4, 23.9, 27.1, 28.6, 45.9, 48.0, 48.8, 126.0, 127.9, 128.3, 146.0
21a	CD_3CN	29.0, 43.7, 125.6, 127.9, 128.0, 146.3
22a[b]	CD_3CN	27.2, 29.0, 43.5, 45.5, 47.7, 49.5, 125.6, 127.9, 128.0, 146.3
23a[b]	$CDCl_3$	27.9, 28.2, 30.3, 47.4, 48.7, 49.1, 51.1, 126.6, 128.5, 128.6, 145.9
24a	$CDCl_3$	28.1, 30.2, 48.2, 49.4, 50.2, 51.6, 126.4, 128.3, 128.4, 145.8
25a	$CDCl_3$	24.6, 30.7, 39.9, 47.3, 49.7, 50.1, 60.1, 126.6, 128.4, 128.5, 145.4
26a[b]	$CDCl_3$	24.8, 28.1, 28.2, 30.2, 47.0, 49.2, 50.2, 51.6, 52.0, 54.0, 54.6, 126.4, 128.1, 128.4, 145.6
27a	$CDCl_3$	27.4,[c] 30.3, 53.8,[c] 126.2, 128.1, 128.6, 145.2
28a	[D_6]DMSO	29.7, 45.9,[c] 125.1, 127.7, 128.2, 146.3
17b	CD_3CN	19.6, 23.6, 45.2, 48.2, 48.4, 129.1, 133.3, 133.4, 135.0
18b	CD_3CN	19.6, 22.7, 45.1, 47.8, 48.2, 58.6, 129.2, 133.3, 133.4, 134.9
19b[b]	CD_3CN	19.6, 24.1, 49.2, 129.2, 133.4, 133.6, 135.3
20b[b,d]	CD_3CN	19.6, 21.7, 24.1, 46.4, 48.0, 48.2, 57.6, 129.2, 133.5, 133.7
21b	CD_3CN	19.6, 43.7, 128.9, 132.5, 133.4, 137.9
22b[b]	CD_3CN	19.6, 27.2, 43.5, 45.4, 47.7, 49.6, 129.0, 132.6, 133.6, 138.2
23b	$CDCl_3$	20.8, 24.9, 27.8, 47.8–51.1,[c] 130.0, 133.8, 134.6, 138.2
24b	$CDCl_3$	20.8, 28.1, 48.0, 49.3, 50.2, 51.7, 129.5, 133.8, 135.0, 137.5
25b[e]	$CDCl_3$	20.8, 24.6, 39.7, 47.3, 49.6, 50.0, 60.2, 129.7, 133.9, 135.0, 137.4 24.0, 24.5, 45.1, 46.0 (2 C), 47.3, 49.0, 50.3, 51.2, 56.2, 62.6
26b[b]	$CDCl_3$	20.8, 24.8, 28.2, 47.0, 49.5, 50.5, 51.6, 52.1, 52.9, 54.0, 54.7, 129.5, 133.7, 134.8, 137.5
27b	$CDCl_3$	20.8, 27.3,[c], 53.7,[c] 129.0, 133.5, 135.1, 136.8
28b	[D_6]DMSO	20.4, 45.5,[c] 128.6, 130.5, 133.8, 142.2

[a] Due to dynamic effects, too many signals were detected for the ring methylene carbon atoms; therefore, only aromatic signals are given. [b] Multiple conformers present; only signals of main component given. [c] br. [d] One aromatic signal not detected due to dynamic processes. [e] Two components due to configuration inversion; ring ligand shifts of the second species (approx. 20%) shown in the second line.

N–*H*) ppm. ^{13}C NMR (62.9 MHz, DMSO): δ = 44.6, 44.8, 45.3, 46.0 ppm. IR: $\tilde{\nu}$ = 3298 m, 2944 m, 2887 m, 1467 m, 1342 w, 1071 vs, 973 s, 945 s, 798 s, 621 vs cm^{-1}.

Preparation of the Thiolate Complexes: The ligand (4 mmol) was added with stirring to 40 mL of a hot 0.1 M solution of $Zn(ClO_4)_2 \cdot 6H_2O$ in methanol. Stirring and heating were continued for an additional 15 min. Depending on the ligand, some precipitation occurred. A solution of 4 mmol of the thiol in 8 mL of 0.5 M KOH was then added dropwise, whereupon potassium perchlorate precipitated. The solution was filtered and, after a varying amount of time, colorless crystals separated spontaneously. The precipitates were filtered off and, if necessary, recrystallized from methanol. All complexes revealed a 1:1:1:1 composition of zinc/macrocyclic amine/thiolate/perchlorate, consistent with the general formula $[Zn(L)(SR)]ClO_4$.

Note: It is important that the precipitation starts as quickly as possible. Prolonged standing of concentrated solutions lowers the yields and the purity of the products considerably, most likely due to oxidation processes. Thus, it is best to induce the formation of crystals by adding a seed crystal or by ultrasound treatment. If the precipitation of the complex occurs instantly upon addition of the potassium thiolate, which is not normally the case, separation from the solid potassium perchlorate is difficult. In such cases, the synthesis should be carried out using a sodium thiolate solution. The desired complex will then be obtained in a good yield, although without the removal of the alkali metal perchlorate.

General Properties and Solubility: All thiolate complexes **17**–**28** form colorless crystalline solids. Substances featuring macrocycles with ring sizes from 14 to 16 atoms and four nitrogen atoms (i.e. **23**–**27**) are readily soluble in chloroform. All complexes, with the exception of **28**, are soluble in acetonitrile and nitromethane, but only partially in methanol. Compounds **28** show only low solubility in all solvents mentioned, but are soluble in DMSO. Other data [elemental analytical data, melting points, and yields (Table 1), IR and mass spectroscopic data (Table 2), and ^{1}H (Table 3) and ^{13}C NMR (Table 4) data] are given in the respective tables.

Crystal Structure Determination:[45] The intensity data for compound **23b** were collected with a Nonius CAD4 diffractometer and for the other compounds with a Nonius KappaCCD diffractometer, using graphite-monochromated Mo-K_α radiation. Data were corrected for Lorentz and polarization effects, but not for absorption.[46–48] The structures were solved by direct methods (SHELXS[49]) and refined by full-matrix least-squares techniques against F_o^2 (SHELXL-97[50]). For all compounds except for **17b**, **19a**, **20a**, and **21b**, the hydrogen atoms of the amine groups were located by difference Fourier synthesis and refined isotropically. All other hydrogen atoms were included at calculated positions with fixed thermal parameters. All non-hydrogen atoms were refined anisotropically.[50] The absolute structures of compounds **16**, **19a**, **21a**, and **28b** could not be determined because they show racemic twinning. XP (SIEMENS Analytical X-ray Instruments, Inc.) was used for structure representations. The drawings in this paper were generated using PLATON.[51]

Acknowledgments

Financial support of this work by the Deutsche Forschungsgemeinschaft (SFB 436: "Metal-Mediated Reactions Modeled After Nature") is gratefully acknowledged.

[1] G. Parkin, *Chem. Rev.* **2004**, *104*, 699–767.
[2] E. Kimura, T. Koike, *Adv. Inorg. Chem.* **1997**, *44*, 229–261.
[3] L. C. Myers, M. P. Terranova, A. E. Ferentz, G. Wagner, G.-L. Verdine, *Science* **1993**, *261*, 1164.
[4] R. G. Matthews, C. W. Goulding, *Curr. Opin. Chem. Biol.* **1997**, *1*, 332–339.
[5] K. Peariso, Z. S. Zhou, A. E. Smith, R. G. Matthews, J. E. Penner-Hahn, *Biochemistry* **2001**, *40*, 987–993.
[6] H.-W. Park, S. R. Boduluri, J. F. Moomaw, P. J. Casey, L. S. Beese, *Science* **1997**, *275*, 1800–1805.
[7] J. J. Wilker, S. J. Lippard, *Inorg. Chem.* **1997**, *36*, 969–978.
[8] R. Burth, H. Vahrenkamp, *Z. Anorg. Allg. Chem.* **1998**, *624*, 381–385.
[9] U. Brand, M. Rombach, J. Seebacher, H. Vahrenkamp, *Inorg. Chem.* **2001**, *40*, 6151–6157.
[10] M. Ji, B. Benkmil, H. Vahrenkamp, *Inorg. Chem.* **2005**, *44*, 3518–3523.
[11] B. S. Hammes, C. J. Carrano, *Inorg. Chem.* **1999**, *38*, 4593–4600.
[12] B. S. Hammes, C. J. Carrano, *Inorg. Chem.* **2001**, *40*, 919–927.
[13] J. N. Smith, Z. Shirin, C. J. Carrano, *J. Am. Chem. Soc.* **2003**, *125*, 868–869.
[14] C. A. Grapperhaus, T. Tuntulani, J. H. Reibenspies, M. Y. Darensbourg, *Inorg. Chem.* **1998**, *37*, 4052–4058.
[15] J. F. Woessner Jr, *FASEB J.* **1991**, *5*, 2145–2154.
[16] H. Nagase, J. F. Woessner Jr, *J. Biol. Chem.* **1999**, *274*, 21491–21494.
[17] H. Matter, M. Schudok, *Curr. Opin. Drug Discovery Dev.* **2004**, *7*, 513–535.
[18] N. Borkakoti, *Biochem. Soc. Trans.* **2004**, *32*, 17–20.
[19] S. P. Salowe, A. I. Marcy, G. C. Cuca, C. K. Smith, I. E. Kopka, W. K. Hagmann, J. D. Hermes, *Biochemistry* **1992**, *31*, 4535–4540.
[20] R. C. Holz, S. P. Salowe, C. K. Smith, G. C. Cuca, L. Que Jr, *J. Am. Chem. Soc.* **1992**, *114*, 9611–9614.
[21] E. B. Springman, E. L. Angleton, H. Birkedahl-Hansen, H. E. Van Wart, *Proc. Natl. Acad. Sci. USA* **1990**, *87*, 364–368.
[22] H. E. Van Wart, H. Birkedahl-Hansen, *Proc. Natl. Acad. Sci. USA* **1990**, *87*, 5578–5582.
[23] B. M. Bridgewater, T. Fillebeen, R. A. Friesner, G. Parkin, *J. Chem. Soc., Dalton Trans.* **2000**, 4494–4496.
[24] D.-W. Christianson, C. A. Fierke, *Acc. Chem. Res.* **1996**, *29*, 331–339.
[25] T. Wingo, C. Tu, P. J. Laipis, D. N. Silverman, *Biochem. Biophys. Res. Commun.* **2001**, *288*, 666–669.
[26] G. Protoschill-Krebs, C. Wilhelm, J. Kesselmeier, *Atmos. Environ.* **1996**, *30*, 3151–3156.
[27] S. Schenk, J. Kesselmeier, E. Anders, *Chem. Eur. J.* **2004**, *10*, 3091–3105.
[28] M. Bräuer, E. Anders, S. Sinnecker, W. Koch, M. Rombach, H. Brombacher, H. Vahrenkamp, *Chem. Commun.* **2000**, 647–648.
[29] M. Rombach, H. Vahrenkamp, *Inorg. Chem.* **2001**, *40*, 6144–6150.
[30] J. E. Richman, T. J. Atkins, *J. Am. Chem. Soc.* **1974**, *96*, 2268–2270.
[31] T. Koike, M. Takamura, E. Kimura, *J. Am. Chem. Soc.* **1994**, *116*, 8443–8449.
[32] A.-W. Addison, E. Sinn, *Inorg. Chem.* **1983**, *22*, 1225–1228.
[33] R. Yang, L.-L. Zompa, *Inorg. Chem.* **1976**, *15*, 1499–1502.
[34] L.-L. Zompa, *Inorg. Chem.* **1978**, *17*, 2531–2536.
[35] M. T. S. Amorim, S. Chave, R. Delgado, J. J. R. F. da Silva, *J. Chem. Soc., Dalton Trans.* **1991**, 3065–3072.
[36] E. K. Barefield, F. Wagner, *Inorg. Chem.* **1973**, *12*, 2435–2439.
[37] R. Luckay, T. E. Chantson, J. H. Reibenspies, R. D. Hancock, *J. Chem. Soc., Dalton Trans.* **1995**, 1363–1367.
[38] F. Wagner, M. T. Mocella, M. J. D'Aniello Jr, A. H.-J. Wang, E. K. Barefield, *J. Am. Chem. Soc.* **1974**, *96*, 2625–2627.
[39] B. Bosnich, C. K. Poon, M. L. Tobe, *Inorg. Chem.* **1965**, *4*, 1102–1108.

[40] N. W. Alcock, P. Moore, C. Pierpoint, *J. Chem. Soc., Dalton Trans.* **1984**, 2371–2376.
[41] J. Marek, P. Kopel, Z. Travnicek, *Acta Crystallogr., Sect. C* **2003**, *59*, 558–560.
[42] D. Swenson, N. C. Baenziger, D. Coucouvanis, *J. Am. Chem. Soc.* **1978**, *100*, 1932–1934.
[43] N. Ueyama, T. Sugawara, K. Sasaki, A. Nakamura, S. Yamashita, Y. Wakatsuki, H. Yamazaki, N. Yasuoka, *Inorg. Chem.* **1988**, *27*, 741–747.
[44] A. Bencini, M. I. Burguete, E. Garcia-Espana, S. V. Luis, J. F. Miravet, C. Soriano, *J. Org. Chem.* **1993**, *58*, 4749–4753.
[45] CCDC-257864 to -257884 contain the supplementary crystallographic data for this paper. These data can be obtained free of charge from The Cambridge Crystallographic Data Centre via http://www.ccdc.cam.ac.uk/data_request/cif.
[46] *MOLEN, An Interactive Structure Solution Procedure*, Enraf–Nonius, Delft, The Netherlands, **1999**.
[47] *COLLECT, Data Collection Software*, Nonius B.V., The Netherlands, **1998**.
[48] Z. Otwinowski, W. Minor, in *Methods in Enzymology* (Eds.: C. Carter, R. Sweet), Academic Press, New York, **1997**, pp. 307–326.
[49] G. Sheldrick, *Acta Crystallogr., Sect. A* **1990**, *46*, 467–473.
[50] G. Sheldrick, *SHELXL-97*, Release 97-2, University of Göttingen, Germany, **1997**.
[51] A. L. Spek, *PLATON, A Multipurpose Crystallographic Tool*, Utrecht University, Utrecht, The Netherlands, **2004** (http://www.cryst.chem.uu.nl/platon).

Received: October 26, 2005
Published Online: February 21, 2006

